Inorganic Chemistry

Communication

pubs.acs.org/IC

Reductive Elimination of Hypersilyl Halides from Zinc(II) Complexes. Implications for Electropositive Metal Thin Film Growth

Chatu T. Sirimanne,[†] Marissa M. Kerrigan,[†] Philip D. Martin,[†] Ravindra K. Kanjolia,[‡] Simon D. Elliott,[§] and Charles H. Winter*[,†]

[†]Department of Chemistry, Wayne State University, Detroit, Michigan 48202, United States

[‡]SAFC Hitech, 1429 Hilldale Avenue, Haverhill, Massachusetts 01832, United States

[§]Tyndall National Institute, University College Cork, Lee Maltings, Cork, Ireland

Supporting Information

ABSTRACT: Treatment of $Zn(Si(SiMe_3)_3)_2$ with ZnX_2 (X = Cl, Br, I) in tetrahydrofuran (THF) at 23 °C afforded $[Zn(Si(SiMe_3)_3)X(THF)]_2$ in 83−99% yield. X-ray crystal structures revealed dimeric structures with Zn_2X_2 cores. Thermogravimetric analyses of $[Zn(Si(SiMe_3)_3)X(THF)]_2$ demonstrated a loss of coordinated THF between 50 and 155 °C and then single-step weight losses between 200 and 275 °C. The nonvolatile residue was zinc metal in all cases. Bulk thermolyses of $[Zn(Si(SiMe_3)_3)X(THF)]_2$ between 210 and 250 °C afforded zinc metal in 97−99% yield, $Si(SiMe_3)_3X$ in 91−94% yield, and THF in 81−98% yield. Density functional theory calculations confirmed that zinc formation becomes energetically favorable upon THF loss. Similar reactions are likely to be general for $M(SiR_3)_n/MX_n$ pairs and may lead to new metal-film-growth processes for chemical vapor deposition and atomic layer deposition.

Thin films of metals have many important applications in microelectronics and magnetic devices.[1] Atomic layer deposition (ALD) is a film-growth technique that provides conformal coverage of nanoscale features and subnanometer control over film thicknesses because of its self-limited growth mechanism.[2] In many future devices, transition metal and other metal films will need to be grown by ALD to meet performance requirements.[1−3] Such ALD growth requires a rapid, complementary reaction between a metal precursor and a reducing coreagent to afford the metal. Considerable progress has been made on the ALD growth of metallic copper and noble metal films[1−3] largely because of the positive electrochemical potentials ($E°$) of ions of these metals and attendant ease of reduction to the metals with a range of reagents.[1−3] By contrast, most other metal ions have negative $E°$ values and are much more difficult to reduce to metals.[1] As such, thermal ALD growth of these metals is difficult and remains poorly developed.[1] H_2 has been the most commonly used as the reducing coreagent to date in ALD,[1,4] but many metal ions have low reactivities toward H_2 at desired ALD growth temperatures of ≤200 °C.[1] We recently reported that $BH_3(NHMe_2)$ serves as a powerful reducing coreagent for nickel(II), cobalt(II), iron(II), chromium(II), and possibly manganese(II) α-imino alkoxide precursors in the ALD growth of these metals at ≤200 °C.[5] However, these processes required a ruthenium substrate to decompose $BH_3(NHMe_2)$ to more a reactive reducing species, and the growth stopped once the film covered the ruthenium surface. Elemental zinc films have been grown by chemical vapor deposition (CVD) at ≥150 °C by thermal decomposition of bis(allyl)zinc.[6] Thermal decomposition of $ZnEt_2$ to zinc metal occurs below 127 °C on many surfaces.[7] Additionally, the use of $ZnEt_2$ as a reducing agent in ALD growth with $Cu(OCHMeCH_2NMe_2)_2$ affords Cu−Zn alloys at ≥120 °C through parasitic thermal decomposition of $ZnEt_2$ to zinc metal.[8] However, no ALD processes for zinc metal have been reported because of a lack of appropriate chemical precursors.

Recently, ALD growth of antimony thin films was demonstrated using $SbCl_3$ and $Sb(SiEt_3)_3$.[9] This process proceeds by elimination of $SiEt_3Cl$ and is a totally new approach for ALD of element films, in this case a nonmetal.[9] Related reactions could represent powerful methodologies for ALD growth of *metallic* first-row transition- and electropositive-metal films and could avoid potential problems associated with H_2 and highly reactive hydride reagents.[1,5] Within this context, we describe a series of reactions that occur upon treatment of bis(hypersilyl)zinc, $Zn(Si(SiMe_3)_3)_2$,[11] with ZnX_2 (X = Cl, Br, I) ultimately to afford zinc metal and $Si(SiMe_3)_3X$. These results demonstrate that reductive eliminations of silyl halides from zinc(II) centers are facile, thus suggesting new, potentially general chemistry for the growth of metal films. Significantly, the electrochemical potential of the Zn^{2+} ion ($E°$ = −0.7618 V[10]) is significantly more negative than that of the Sb^{3+} ion ($E°$ = 0.152 V[10]), implying that silyl halide reductive eliminations may provide general access to many electropositive metals.

$Zn(Si(SiMe_3)_3)_2$ was prepared according to a literature procedure[11a] and treated with 1 equiv of ZnX_2 (X = Cl, Br, I) in tetrahydrofuran (THF; Scheme 1). No color changes or precipitation occurred upon mixing at ambient temperature or refluxing for 18 h. Analysis of these reaction mixtures after stirring at 23 °C for 3 h indicated the formation of products **1**−**3**, as outlined in Scheme 1. Complexes **1**−**3** were isolated by crystallization and were characterized by spectral and analytical data and by X-ray crystallography.[12] The ^1H and $^{13}C\{^1H\}$ NMR spectra revealed the expected resonances for the $Si(SiMe_3)_3$ and THF ligands, and the former resonances were shifted from those

Received: September 8, 2014
Published: December 9, 2014

   dx.doi.org/10.1021/ic502184f | Inorg. Chem. 2015, 54, 7−9

Scheme 1. Synthesis and Thermolysis of 1−3

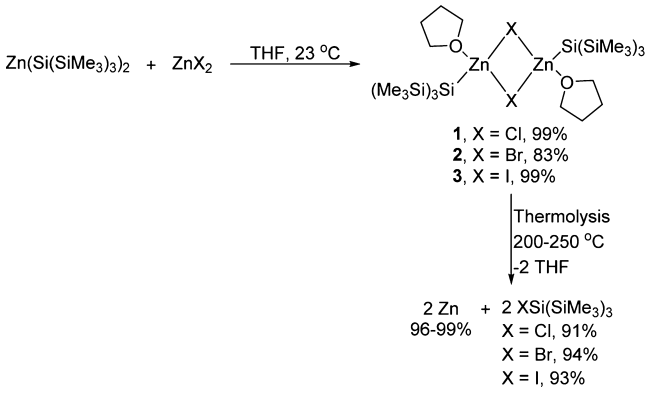

of $Zn(Si(SiMe_3)_3)_2$. Complex **1** was previously reported using a different synthetic method.[13] Complexes **1**−**3** have similar dimeric structures, with one $Si(SiMe_3)_3$ and one THF ligand per zinc ion and two halide ions that bridge between the zinc ions. The $Si(SiMe_3)_3$ groups are anti to each other within the dimers, to avoid steric crowding. Figure 1 shows a perspective view of **2**. The Zn−Br, Zn−Si, and Zn−O bond lengths are 2.5030(6) and 2.5382(6), 2.352(1), and 2.101(3) Å, respectively.

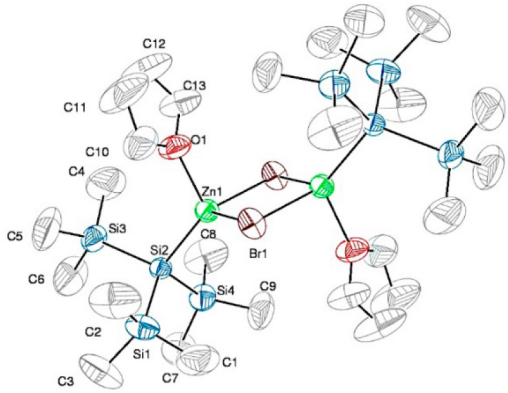

Figure 1. Perspective view of **2** with thermal ellipsoids at the 50% level. Selected bond lengths (Å) and angles (deg): Zn−Br 2.5030(6), Zn−Br′ 2.5382(6), Zn−Si2 2.352(1), Zn−O1 2.101(3); Zn−Br−Zn′ 81.16(2), Br−Zn−Br′ 93.84(2), Br−Zn−Si2 124.52(3), Br−Zn′−Br′ 121.70(3), Br−Zn−O 96.88(9), Br′−Zn−O 94.56(9).

Thermogravimetric analyses (TGA) of **1**−**3** were carried out to understand their solid-state decompositions. The THF ligands are labile, and their loss was observed starting at 50 °C and was complete by 155 °C. Then, single-step weight losses occurred between 200 and 275 °C to afford 11.67, 6.02, and 3.84% weight residues for **1**−**3**, respectively. The percentages of zinc in **1**−**3** are 15.55, 14.06, and 12.77%, respectively. The lower observed residues, compared to those predicted by the percentage of zinc in **1**−**3**, may originate from partial sublimation of **1**−**3** or the THF-free products thereof.

Encouraged by the TGA data, we next explored solid-state thermolyses of **1**−**3**.[12] Pressure tubes fitted with Teflon stoppers were charged with ∼0.4 mmol each of **1**−**3** and hexamethylbenzene as an internal standard. These tubes were then heated at 210 (**1**), 225 (**2**), and 250 °C (**3**) for 4 h. During the thermolyses, the white solids gradually transformed to granular gray solids and colorless liquids condensed at the cool area near the Teflon stoppers. Workup entailed extraction of the flask contents with benzene-d_6, decanting of the extracts, and vacuum drying of the gray powders. Powder X-ray diffraction revealed the gray powders to be zinc metal, with isolated yields of 96−99%.[12] ^{1}H and $^{13}C\{^1H\}$ NMR spectra of the extracts showed that the soluble products were $Si(Si(CH_3)_3)_3X$ (91−94%) and THF (81−98%), based on a comparison with the NMR data of authentic samples.[12]

Density functional theory (DFT) calculations using *VASP*[14] and *TURBOMOLE*[15] were used to predict the structures of intermediates and quantify the changes in bonding, as detailed in the Supporting Information.[12] The gas-phase compounds $[Zn(Si(SiMe_3)_3)Cl]_n$ increase in stability upon oligomerization, with $n = 4$ predicted to be the most stable [$\Delta E = -49.1$ kJ/mol of zinc relative to $ZnCl_2$ and $Zn(Si(SiMe_3)_3)_2$]. The tetramer is predicted to contain a cubic Zn_4Cl_4 core. The X-ray crystal structure of $[Zn(Si(tBu)_3)Br]_4$ has been reported[16] and exists with a cubic Zn_4Br_4 core, thus supporting the DFT calculations of $[Zn(Si(SiMe_3)_3)Cl]_4$. However, it is not clear if the tetramer is accessible after THF loss in the current experiments. Thermolysis of solid **2** at 111 °C and 0.05 Torr for 24 h in a drying tube afforded a THF-free complex of the apparent formula $[Zn(Si(SiMe_3)_3)Br]_x$;[12] however, X-ray-quality crystals could not be obtained despite multiple attempts, and the compound was not pursued further.

The DFT calculations revealed that the formation of THF adducts from $[Zn(Si(SiMe_3)_3)Cl]_n$ is thermodynamically favorable for n = 1−3. For formation from $ZnCl_2$, $Zn(Si(SiMe_3)_3)_2$, and THF, the dimer $[Zn(Si(SiMe_3)_3)Cl(THF)]_2$ is computed to be the most stable ($\Delta E = -68.4$ kJ/mol of zinc neglecting entropy), consistent with the isolation of **1**−**3**. However, the trimer $[Zn(Si(SiMe_3)_3)Cl(THF)]_3$ is predicted to be only <2 kJ/mol less stable than the dimer. The calculated Zn−Cl (2.40−2.43 Å) and Zn−Si (2.39 Å) distances in the dimer are within 2% of those observed in the X-ray crystal structure of **1** [2.391(2) and 2.347(2) Å], which is within the accuracy of DFT.

We next used DFT to predict the thermodynamic stabilities of various zinc complexes toward elimination of $Si(SiMe_3)_3X$. Consistent with the high stabilities of **1**−**3** documented above, the THF-coordinated dimer **1** is thermodynamically stable by +22 kJ/mol of zinc at 0 K with respect to the reductive elimination of $Si(SiMe_3)_3Cl$ and the production of zinc metal. However, a loss of THF ligands causes the resulting THF-free $[Zn(Si(SiMe_3)_3)Cl]_2$ to become metastable by −12.5 kJ/mol of zinc toward the reductive elimination of $Si(SiMe_3)_3Cl$ and the formation of zinc metal. Because entropy has been neglected, this energy difference (+22 → −12.5 kJ/mol) reflects metastable bonding within the complex. Similar switches to metastability upon a loss of THF ligands are computed for the monomer $Zn(Si(SiMe_3)_3)Cl(THF)$ (+14.4 → −45.9 kJ/mol of zinc) and trimer $[Zn(Si(SiMe_3)_3)Cl(THF)]_3$ (+20.9 → −12.5 kJ/mol of zinc). The metastability toward reductive elimination is likely due to lower coordination numbers at zinc upon THF loss. These observations are consistent with experiment because the TGA data reveal that THF loss from **1**−**3** occurs prior to decomposition. By contrast, reductive elimination from the tetramer $[Zn(Si(SiMe_3)_3)Cl]_4$ is not favored, apparently because each zinc ion is four-coordinate and thus coordinatively saturated, although the small energy cost (ΔE = +2.9 kJ/mol of zinc) can probably be overcome at elevated temperatures.

The overall reaction $Zn(Si(SiMe_3)_3)_2 + ZnCl_2 \rightarrow 2Zn + 2Si(SiMe_3)_3Cl$ is computed by DFT to show $\Delta E = -46$ kJ/mol of zinc and $\Delta G = -52$ kJ/mol of zinc at T = 100 °C, indicating that it is a thermodynamically viable route to the ALD of zinc.

dx.doi.org/10.1021/ic502184f | *Inorg. Chem.* 2015, 54, 7−9

This prediction is consistent with the observed decompositions of **1**−**3** upon thermolysis. For reference, analogous DFT calculations of the ALD reaction for the deposition of antimony from $SbCl_3$ and $Sb(SiEt_3)_3$[9] predict a favorable ΔE value of −140 kJ/mol of antimony.[12] The highest occupied molecular orbital of $Zn(Si(SiMe_3)_3)_2$ is found to be Si−Zn−Si σ bonding, and this is the ultimate source of electrons that reduce the zinc ion to metallic form. The $[Zn(Si(SiMe_3)_3)Cl]_n$ clusters also show $2n$ electrons in high-lying σ(Zn−Si) orbitals that become available for the reduction of zinc when the Zn−Si bond is broken. At the same time, the ligating silicon atoms of the hypersilyl groups become oxidized. The DFT calculations reveal a similar role for σ(Sb−Si) bonding orbitals in $Sb(SiEt_3)_3$.

This work has several implications for the growth of metal films by CVD and ALD using silyl halide elimination reactions. Most importantly, reductive elimination of $Si(SiMe_3)_3X$ is predicted to be energetically favorable for the zinc(II) ion, although no prediction about kinetics can be made without knowledge of a reaction pathway in solution or during ALD. The formation of zinc metal from **1**−**3** demonstrates favorable reactions at 210−250 °C. The metastable unsolvated adducts $[ZnSi(SiMe_3)_3Cl]_n$ are representative of structures that might form on the growing surface in a potential film growth process using $ZnCl_2$ and $Zn(Si(SiMe_3)_3)_2$, which implies that the present work may lead to a zinc metal ALD process. In this vein, $Zn(Si(SiMe_3)_3)_2$ sublimes at 110 °C and 0.05 Torr, decomposes thermally at about 350 °C, and thus has excellent ALD precursor properties.[12] Virtually all ALD processes for zinc-containing films use $ZnEt_2$ as a precursor,[17] and our calculations predict ΔE = −103 kJ/mol of zinc for the reaction $Zn(Si(SiMe_3)_3)_2 + ZnEt_2 \rightarrow 2Zn + 2Si(SiMe_3)_3Et$.[12] This is even more exothermic than the formation of zinc metal from $ZnCl_2$ and $Zn(Si(SiMe_3)_3)_2$ and may be a promising ALD approach if the depositions proceed at or below the thermal decomposition temperature of $ZnEt_2$ (∼130 °C).[7,8] The favorable energetics with $ZnEt_2$ suggest that precursors other than metal halides can likely be used. However, more volatile and thermally stable zinc precursors need to be developed. Finally, zinc is an excellent model for first-row transition metals because its metal radius is about the same as those of vanadium and chromium, the $E°$ value of the zinc(II) ion ($E°$ = −0.74 V[10]) lies between those of iron(II) ($E°$ = −0.44 V[10]) and chromium(II) ($E°$ = −0.94 V[10]), and the coordination chemistry of zinc(II) is similar to first-row transition-metal(II) ions. Analogous reactions of $M(SiR_3)_n$[18] and MX_n are likely to afford metals and should be similarly exothermic, which may lead to new growth processes for metal films upon appropriate precursor development.

■ ASSOCIATED CONTENT

Supporting Information

Synthetic procedures and analytical and spectroscopic data for **1**−**3**, X-ray crystallographic data for **1**−**3** in CIF format, and details of the DFT calculations. This material is available free of charge via the Internet at http://pubs.acs.org.

■ AUTHOR INFORMATION

Corresponding Author

*E-mail: chw@chem.wayne.edu.

Notes

The authors declare no competing financial interest.

■ ACKNOWLEDGMENTS

We are grateful to the U.S. National Science Foundation (Grant CHE-1212574), Science Foundation Ireland (Grant 09/IN.1/I2628), and SAFC Hitech for support of this research.

■ REFERENCES

(1) (a) Knisley, T. J.; Kalutarage, L. C.; Winter, C. H. *Coord. Chem. Rev.* **2013**, *257*, 3222−3231. (b) Ramos, K. B.; Saly, M. J.; Chabal, Y. J. *Coord. Chem. Rev.* **2013**, *257*, 3271−3281. (c) Emslie, D. J. H.; Chadha, P.; Price, J. S. *Coord. Chem. Rev.* **2013**, *257*, 3282−3296. (d) Leskelä, M.; Ritala, M.; Nilsen, O. *MRS Bull.* **2011**, *36*, 877−884.

(2) (a) George, S. M. *Chem. Rev.* **2010**, *110*, 111−131. (b) Leskelä, M.; Ritala, M. *Angew. Chem., Int. Ed.* **2003**, *42*, 5548−5554. (c) Putkonen, M.; Niinistö, L. *Top. Organomet. Chem.* **2005**, *9*, 125−145.

(3) Hämäläinen, J.; Ritala, M.; Leskelä, M. *Chem. Mater.* **2014**, *26*, 786−801.

(4) Lim, B. S.; Rahtu, A.; Gordon, R. G. *Nat. Mater.* **2003**, *2*, 748−754.

(5) Kalutarage, L. C.; Martin, P. D.; Heeg, M. J.; Winter, C. H. *J. Am. Chem. Soc.* **2013**, *135*, 12588−12591.

(6) Cheon, J.; Dubois, L. H.; Girolami, G. S. *Chem. Mater.* **1994**, *6*, 2279−2287.

(7) (a) Rueter, M. A.; Vohs, J. M. *Surf. Sci.* **1992**, *262*, 42−50. (b) Kovacs, I.; Iost, N.; Solymosi, F. *J. Chem. Phys.* **1994**, *101*, 4236−4247.

(8) (a) Vidjayacoumar, B.; Emslie, D. J. H.; Clendenning, S. B.; Blackwell, J. M.; Britten, J. F.; Rheingold, A. *Chem. Mater.* **2010**, *22*, 4844−4853. (b) Lee, B. H.; Hwang, J. K.; Nam, J. W.; Lee, S. U.; Kim, J. T.; Koo, S.-M.; Baunemann, A.; Fischer, R. A.; Sung, M. M. *Angew. Chem., Int. Ed.* **2009**, *48*, 4536−4539.

(9) Pore, V.; Knapas, K.; Hatanpää, T.; Sarnet, T.; Kemell, M.; Ritala, M.; Leskelä, M.; Mizohata, K. *Chem. Mater.* **2011**, *23*, 247−254.

(10) *Handbook of Chemistry and Physics*, 92nd ed.; CRC Press: Boca Raton, FL, 2011−2012; pp 5-80−5-89, http://www.hbcpnetbase.com/.

(11) (a) Arnold, J.; Tilley, T. D.; Rheingold, A. L.; Geib, S. J. *Inorg. Chem.* **1987**, *26*, 2106−2109. (b) Gaderbauer, W.; Balatoni, I.; Wagner, H.; Baumgartner, J.; Marschner, C. *Dalton Trans.* **2010**, *39*, 1598−1603.

(12) See the Supporting Information.

(13) Nanjo, M.; Oda, T.; Mochida, K. *J. Organomet. Chem.* **2003**, *672*, 100−108.

(14) Kresse, G.; Furthmüller, J. *Phys. Rev. B* **1996**, *54*, 11169.

(15) Ahlrichs, R.; Bär, M.; Häser, M.; Horn, H.; Kölmel, C. *Chem. Phys. Lett.* **1989**, *162*, 165.

(16) Wiberg, N.; Amelunxen, K.; Lerner, H.-W.; Nöth, H.; Appel, A.; Knizek, J.; Polborn, K. *Z. Anorg. Allg. Chem.* **1997**, *623*, 1861−1870.

(17) (a) Malm, J.; Sahramo, E.; Perälä, J.; Sajavaara, T.; Karppinen, M. *Thin Solid Films* **2011**, *519*, 5319−5322. (b) Makino, H.; Miyake, A.; Yamada, T.; Yamamoto, N.; Yamamoto, T. *Thin Solid Films* **2009**, *517*, 3138−3142.

(18) (a) Nakamoto, M.; Yamasaki, T.; Sekiguchi, A. *J. Am. Chem. Soc.* **2005**, *127*, 6965−6955. (b) Heyn, R. H.; Tilley, T. D. *Inorg. Chim. Acta* **2002**, *341*, 91−98. (c) Farwell, J. D.; Lappert, M. F.; Marschner, C.; Strissel, C.; Tilley, T. D. *J. Organomet. Chem.* **2000**, *603*, 185−188. (d) Klett, J.; Klinkhammer, K. W.; Niemeyer, M. *Chem.—Eur. J.* **1999**, *5*, 2531−2536.